

COVER PAGE

Document downloaded by @DAEL

Thu Nov 26 23:47:38 2026
For personal use

When automatic English translation is provided, only the original document is authentic.
The EAA cannot be held responsible of any translation error

Bibliographical reference

Signal Loss of Reflected and Transmitted Ultrasonic Waves Induced by Double Rough Interfaces, Zi-Qiang Chen and Lin Yang, Acta Acustica **vol. 96** (Number 5), 2010, pp. 823-830

DOI
https://doi.org/10.3813/AAA.918340

ACTA ACUSTICA UNITED WITH ACUSTICA
Vol. 96 (2010) 823 – 830
DOI 10.3813/AAA.918340

Signal Loss of Reflected and Transmitted Ultrasonic Waves Induced by Double Rough Interfaces

Zi-qiang Chen, Lin Yang
School of Mechanics and Power Engineering, Shanghai Jiao Tong University, Shanghai 200240, P.R. China.
chenziqiang@situ.edu.cn

Summary
A simple analytical model evaluating the signal loss of reflected and transmitted ultrasonic waves induced by double random rough interfaces was presented based on the Phase-Screen approximation (PSA). By expressing the phase correlation factor of the acoustic beam doubly transmitting through rough interfaces into the function of the flaw depth and the incident angle, the model overcomes some limitations and inadequacy subjected by those models which use only the phase-screen approximation to evaluate the signal loss of waves induced by the single rough interface. The signal attenuation will decrease with the increase of the beamŠs incident angle for the flaw near the upper interface, while the signal attenuation is not sensitive to the incident angle, as the flaw is far from the upper interface. The results indicate that the influence of the angle factor for the waves doubly transmitted through the rough interface on the phase correlation will only operate near the upper interface. The experimental results show that the theoretical prediction is in good agreement with experimental measurements. Therefore, the model proposed in the paper is suitable for the real-time ultrasonic non-destructive testing of rough flaws under the rough surfaces in materials.

PACS no. 43.25.-x, 43.58. e

1. Introduction

The scattering of acoustic and electromagnetic waves from random or periodic rough interfaces has been an active area of research for decades, in radar, sonar, non-destructive evaluation (NDE) applications, and diagnostic ultrasound. In particular, the inspection of components such as cylinder cover of engine that contain cracks and imperfect interfaces has always been among the most significant issues in the NDE of materials. Specifically, operating in the pulse-echo mode [1, 2, 3] or based on the elastodynamic theory [4] or using the time delay spectrometry [5] or the time-reversal technique [6], the ultrasound can be used to characterize surface parameters of rough interfaces such as the root-mean-square (rms) roughness.

The rough interface appears in not only surfaces of object, but also in interior of materials, such as the rough crack [7], the soldering interface, the friction welding interface, the viscera surface, etc. The rough interface will influence the field of refection, transmission or backscattering greatly, and randomize the phase of the acoustic beam. Therefore, rough interface will worsen the acoustic wave signal remarkably. To improve the reliability of non-destructive testing (NDT), the interaction of an acoustic wave with rough interface between two different media is still of considerable interest in recent years [8, 9, 10, 11]. For relieving the computational burden, an analytical approach has been provided for analyzing the behavior of guided waves (Lamb-type waves) propagating inside plates with a rough surface [12, 13].

Nagy and Adler [14] set up a model by using Phase–Screen approximation (PSA) to study the influence of rough surface on the average transmission field when the acoustic waves impinge the rough surface at a right angle. The theory uses a transmission coefficient depending on frequency and root-mean-square roughness to replace one of the smooth surfaces. Nagy and Rose [15] measured and calculated the transmission coefficient of the average acoustic field through rough surfaces, and considered the oblique incidence of the beam. They found out that the PSA can describe the acoustic signal accurately at any incident angle except in the critical angle. Whereas the multi-interaction of acoustic waves with rough interfaces have not been considered in these models.

In this paper, a simple analytical model for evaluating the signal loss of reflected and transmitted ultrasonic waves induced by double random rough interfaces is established for the real-time inspection of flaws in materials through ultrasonic imaging systems.

In the rest of this paper, section 2 introduces the geometry of double random rough surfaces and some basic

Received 24 February 2009,
accepted 1 May 2010.

© S. Hirzel Verlag · EAA

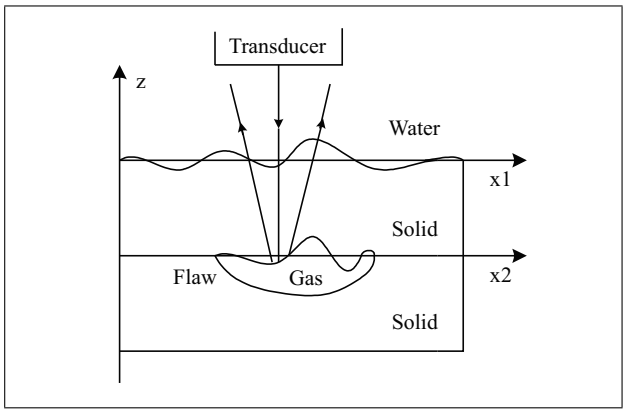


Figure 1. Schematic diagram of double random rough interfaces.

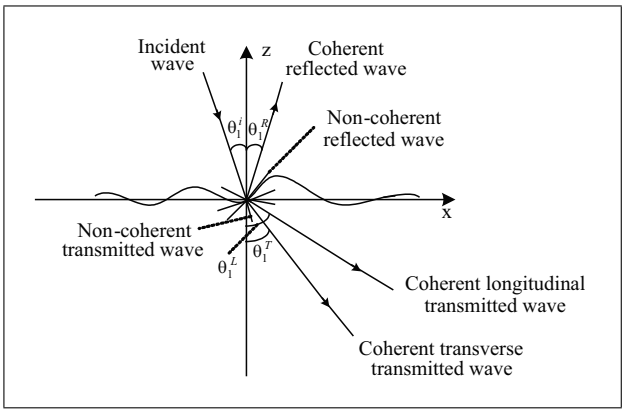


Figure 2. Ultrasonic waves scattering from random rough liquid-solid interfaces.

conceptions of the wave field. Section 3 describes the theoretical derivation of the proposed model. Signal evaluation and discussion are presented in section 4. Experimental validation for the theoretical model is given in the section 5, followed by conclusions in section 6.

2. Geometry and basic conceptions

The Schematic diagram of double random rough surfaces is shown in Figure 1. The whole procedure of the ultrasonic waves scattering from the double random rough surfaces is described as follows. A single ultrasonic wave, propagating through water and impinging the random rough liquid-solid interface at angle θ_1^i, can produce:

- a coherent reflected wave returning to the water;
- a coherent longitudinal transmitted wave to the solid;
- a coherent transverse transmitted wave to the solid;
- a variety of non-coherent scattering waves including reflected and transmitted waves,

as shown in Figure 2. When a single wave impinges the random rough flaw surface (assumed to be solid-gas interface here) at angle θ_2^i, the interaction will produce a coherent longitudinal reflected wave, a coherent transverse reflected wave, and a variety of non-coherent reflected (scattering) waves, as shown in Figure 3. The coherent waves are the mean valued component, while the non-coherent waves are randomly fluctuating components. Actually, the non- coherent scattering waves (noise) are generated by the backscatter from some grains in anisotropic materials. It has been shown that the surface roughness attenuates the backscattered non-coherent noise much less than the coherent waves do [16]. Moreover, based on the assuming of isotropic materials used in the paper, the component of non-coherent scattering waves is much less than that of coherent waves. Therefore only the signal loss of coherent waves is taken into consideration and the influence of non-coherent scattering waves on the signal loss will be neglected in this paper.

When the ultrasonic wave impinges the liquid-solid interface (upper interface) at angle θ_1^i, the transmitting angles of longitudinal (L) wave and transverse (T) wave are

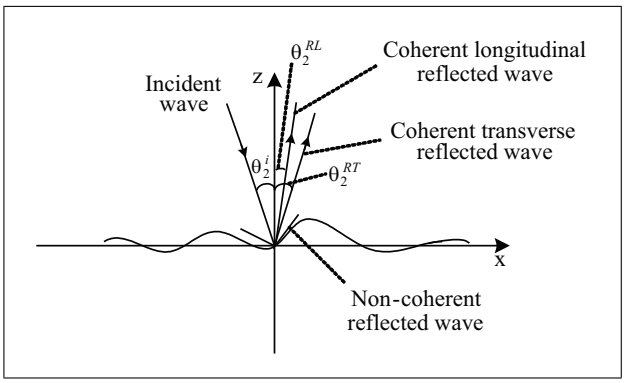


Figure 3. Ultrasonic waves scattering from random rough solid-gas interfaces.

denoted as θ_1^L and θ_1^T, while the reflecting angle of reflected wave R^1 are given by θ_1^R. The values of reflecting angle and transmitting angle are determined by Snell theorem. As the signals for NDT are longitudinal waves, it can be acquired through the time gating approach of ultrasonic imaging testing systems (UITS). The reflecting angles of the longitudinal reflected wave and the transverse reflected wave are denoted as θ_2^{RL} and θ_2^{RT}, when the longitudinal transmitted wave impinges the solid-gas rough flaw surface (lower interface) at the incident angle $\theta_2^i = \theta_1^L$. The signals UITS needs are still longitudinal waves. Thereafter the longitudinal reflected wave propagates in the solid, and then returns to the solid-water rough interface at an incident angle $\theta_3^i = \theta_2^{RL} = \theta_1^L = \theta_2^i$, and produces the longitudinal transmitted wave with angle $\theta_3^L = \theta_1^i$. Finally, the longitudinal transmitted wave is received by the phase-coherent transducer.

Seen from Figure 1, the geometry consists of a randomly rough liquid-solid (upper) interface and a randomly rough solid-gas (lower) interface positioned in the $z = 0$ plane and $z = d$ plane of a rectangular coordinate system. The sound velocity in water is denoted as c_w, while the sound velocity of longitudinal and transverse wave in the solid are denoted as c_L and c_T, and the angular frequency is denoted as ω. The wave numbers in water and the solid are given as k_w, k_L, and k_T. The random rough upper in-

terface and the lower interface are planar on average at $z = 0$ and $z = d$, respectively. The variation of the rough interface height, $h(r)$, is governed by a spatially uniform, zero-mean Gaussian random process and autocorrelation function $W(r)$. The vector $\boldsymbol{r} = (r_x, r_y, 0)$ represents the variation of location in the x–y plane. The coordinate parallel to the surface is denoted as r, while the general three-dimensional coordinate is $\boldsymbol{x} = (r, z)$. Denoting the height of the two local rough interfaces as $h_1(x, y)$ and $h_2(x, y)$, there is

$$\big\langle h_1(x, y)\big\rangle = 0 \quad \text{and} \quad \big\langle h_2(x, y)\big\rangle = 0, \tag{1}$$

where the $\langle..\rangle$ denotes an average over a hypothetical ensemble of samples with different realizations of the surface roughness. Because the variation of the roughness is assumed to be static random process and is ergodic, the ensemble average is identical with a spatial average over the rough surface. Denoting the rms heights of the two local rough interface as $h_1^2 = \langle h_1^2(x, y)\rangle$ and $h_2^2 = \langle h_2^2(x, y)\rangle$, the assumption of translational invariance implies that the normalized autocorrelation function can be written in the form

$$W_{1,2}(r_{1,2} - r'_{1,2}) \equiv \frac{\big\langle h_{1,2}(r_{1,2}) h_{1,2}(r'_{1,2})\big\rangle}{h_{1,2}^2}. \tag{2}$$

As a Gaussian function, the autocorrelation function can be expressed by

$$W(r - r') = \exp\Big(- \frac{|r - r'|^2}{L_a^2}\Big), \tag{3}$$

where L_a denotes the autocorrelation length, which is defined as the length that the W falls to e^{-1}. Actually, L_a is equivalent to the average diameter of the dents on the rough surface. Because the rms height is much less than the autocorrelation length, the two interfaces are both the small ramp rough interfaces.

Denoting the incident wave field as $U_0^{R,L,T}$, the phase factor as $\phi^{R,L,T}$, the scattering wave field from the rough interface satisfying the condition $h \ll \lambda < L_a$ (λ enotes the wavelength in propagating media) can be expressed as

$$U^{R,L,T} = U_0^{R,L,T} \exp\big(\mathrm{i}\phi^{R,L,T}\big). \tag{4}$$

Equation (4) is just the theoretical expression of PSA which can be deduced and improved from Kirchhoff theorem [17]. As a theory of physical optics, Kirchhoff theorem is also the fundamental for characterizing the acoustic wave field from rough surfaces. Taking the rough surface as a thin phase screen, PSA considers the rough surface as a random modulation or perturbation to the phase of the incident wave.

3. Theoretical derivation

The reflection and transmission coefficients of smooth interface are the mapping of the unit time-harmonious infinite planar wave impinging the smooth infinite planar interface. The reflection and transmission coefficients of the smooth upper interface are denoted as $R_{1,3}^L$, $T_{1,3}^L$ and $T_{1,3}^T$, while the reflection coefficient of the smooth lower interface are given as R_2^L and T_2^T. Here, subscript 1 in the symbols of reflection and transmission coefficients denotes the wave propagating through the upper interface for the first time, subscript 2 denotes the wave propagating through the lower interface, and subscript 3 denotes the wave propagating through the upper interface for the second time after the wave reflecting from the lower interface. According to PSA, the amplitude is a factor slowly varying forward when the acoustic wave propagates through the rough interface, while the phase is a factor varying fast and changing exponentially. Therefore, the entire variation of the pressure wave field in water (denoted by $U_0(\omega, x, y, z)$) will be controlled by the phase variation.

Assuming the pressure wave incident through a rough interface is dependent on two factors: the wave related to the smooth interface and the phase factor related to the local rough interface height, and neglecting the variation of amplitude, and meeting the condition $h \ll \lambda < L_a$, the wave field for the interaction of incident wave with upper rough interface can be expressed as

$$U_1^L(\omega, x, y, z = 0^-) = T_1^L U_{01}^L(\omega, x, y, z) \exp\big[\mathrm{i}\phi_1^L(\omega, x, y)\big], \tag{5}$$

$$U_1^T(\omega, x, y, z = 0^-) = T_1^T U_{01}^T(\omega, x, y, z) \exp\big[\mathrm{i}\phi_1^T(\omega, x, y)\big], \tag{6}$$

$$U_1^R(\omega, x, y, z = 0^+) = R_1 U_{01}^R(\omega, x, y, z) \exp\big[\mathrm{i}\phi_1^R(\omega, x, y)\big], \tag{7}$$

where U_1^L denotes the longitudinal transmission pressure wave from the upper interface, U_1^T is the transverse transmission pressure wave from the upper interface, U_1^R is the reflection pressure wave from the upper interface, and U_{01} is the wave from smooth interface. "0^+" expresses that the beam is immediately above the sampleŠs rough water-solid interface (in the water), and "0^-" expresses that the beam is immediately under the sample's rough water-solid interface (in the solid). Neglecting the additional refraction brought by the rough interface, similar to the route difference of radial optics, the phase variation about the sound wave propagating through the upper interface can be expressed as

$$\phi_1^R = -2h_1(x, y) k_w \cos\theta_1^i, \tag{8}$$

$$\phi_1^{L,T} = -h_1(x, y)\big[k_{L,T} \cos\theta_1^{L,T} - k_w \cos\theta_1^i\big]. \tag{9}$$

Assuming isotropic of the solid sample's materials, neglecting its influence on the sound wave, and combining U_1^L and its longitudinal reflecting wave from the flaw surface, the wave field of secondly propagating through the upper rough interface can be obtained. Thereupon the total pressure wave field of the acoustic wave from incidence to return to the transducer can be obtained,

$$U = R_2^L T_1^L T_3^L U_0 \exp\big(\mathrm{i}\phi_1^L\big) \exp\big(\mathrm{i}\phi_2^{RL}\big) \exp\big(\mathrm{i}\phi_3^L\big) \tag{10}$$

where ϕ_2^{RL} and ϕ_3^L can be given as

$$\phi_2^{RL} = -2h_2(x, y) k_L \cos\theta_1^L \tag{11}$$

and

$$\phi_3^L = -h_1'(x, y)\left[k_w \cos\theta_1^L - k_L \cos\theta_1^L\right]. \quad (12)$$

Taking the ensemble average to the U, there is:

$$\langle U\rangle = R_2^L T_1^L T_3^L U_0 \left\langle \exp\left(\mathrm{i}\phi_1^L\right)\right\rangle \left\langle \exp\left(\mathrm{i}\phi_3^L\right)\right\rangle. \quad (13)$$

The rough interface with Gaussian distribution can be written as

$$\left\langle \exp\left(\mathrm{i}\phi_1 \exp\left(\mathrm{i}\phi_3^L\right)\right)\right\rangle = \exp\left(\sigma^2\right) \exp\left[-\sigma^2 W_1(r_1 - r_1')\right], \quad (14)$$

where σ^2 is

$$\sigma^2 = \left\langle \phi_{1,3}^2 \right\rangle = h_1^2\left(k_L \cos\theta_1^L - k_w \cos\theta_1^1\right)^2. \quad (15)$$

In Equation (13), the former four items express the wave field of smooth interface. The fifth item is the influence factor of lower rough interface, and the last item is the influence factor of upper rough interface. Then the reflection coefficient modulated from upper and lower rough interfaces can be expressed as

$$R^L = R_0^L \exp\left(-2h_2^2 k_L^2 \cos^2\theta_1^L\right) \exp\left[-h_1^2\left(k_L \cos\theta_1^L - k_w \cos\theta_1^i\right)^2\right] \exp\left[-h_1^2\left(k_L \cos\theta_1^L - k_w \cos\theta_1^i\right)^2 \exp\left(-|r_1 - r_1'|^2/L_a^2\right)\right], \quad (16)$$

where R_0^L is the reflection coefficient of the sound wave from incidence to return to the transducer for the smooth interface, $k = 2\pi/(\lambda = \omega/c = 2\pi f/c$ is the wave number.

4. Signal evaluation and discussion

When the acoustic waves impinge the water-solid rough interfaces at an angle near right, the transmitted waves are mainly the longitudinal waves. The longitudinal wave will turn to surface wave and the refraction angle of transverse wave will come to 45° on increasing the incidence angle to a degree (18.6°for the water-copper interface). The signal attenuation can be expressed in the form of dB,

$$Q(\omega, h, c_w, c_L, \theta) = -20\log_{10}\frac{R^L}{R_0^L}. \quad (17)$$

According to the Snell theorem, substitute $k = \omega/c$ to equation (16), and follow equation (17), then the total signal attenuation induced by double rough interfaces can be expressed as

$$Q(\omega, h, c_w, c_L, \theta) = 8.687\omega^2\left\{2h_2^2\frac{1}{c_L^2}\cos^2\theta^L + h_1^2\left(\frac{1}{c_L}\cos\theta^L - \frac{1}{c_w}\cos\theta^i\right)^2 \left[1 + \exp\left[-\frac{-d^2(4\tan^2\theta^L + \sqrt{d}}{L_a^2}\right]\right]\right\}. \quad (18)$$

Seen from equation (18), the signal loss is related to not only the frequency, rms height and sound velocity in the medium, but also the angle and the flaw depth under the upper interface.

The signal loss dependent on the flaw depth is the problem of phase correlation of coherent wave doubly propagating through the upper interface. The value of the phase correlation is determined by the correlation function. While the correlation function is dependent on the flaw depth, the distance of two points in the x-axes after the wave doubly propagated through the upper interface, and the incident angle θ^i or the transmitting angle θ^L of the wave. The correlation will reach maximum (the value of correlation function equals 1) when the flaw depth is zero. In the case of a small incident angle θ^L and a definite correlation length L_a, the signal loss will decrease along with the increase of the flaw depth. This means that the signal loss of flaw near the upper interface is greater than the signal loss of the flaw far from the upper interface. When increases, the long distance flaw signal is almost unaffected by the phase correlation of coherent wave doubly propagating through upper rough interface except for the short-distance flaw signal loss varying obviously, because the value of correlation function is almost zero in this case.

In addition, the autocorrelation length L_a of rough interface represents the peak-to-peak spacing of rough surfaces. The signal loss will increase along with the decrease of La. This means that the amount of coherent waves decrease comparatively. The theorem of PSA will become invalid when $L_a < \lambda$. The comparison of PSA and the second order disturbance approximation [18] shows that the two theorems are both valid only when the longitudinal transmitted waves are within critical angle (otherwise the longitudinal transmitted waves will escape from the medium) and the transverse transmitted waves are in outside the critical angle. The transmission coefficient of rough interface is almost uninfluenced by the solid-liquid density ratio.

Although some interaction factors of acoustic waves with rough interface are neglected, the theorem of PSA is still valid as long as satisfying the condition of $L_a > \lambda \gg h$. Generally, a majority of ultrasonic non-destructive evaluations can meet the conditions, such as the ultrasonic testing of smooth flaws or flaws with little roughness under rough metal surfaces. But for the flaws with large roughness, such as some cracks in some range of dimension and shape, could only meet it partly.

For the friction welding and soldering interface with flaws, such as cracks, poor penetrations, slag inclusions, etc., the interfaces are generally rather thin to meet the condition $h \ll L_a$, therefore the model of this paper about the signal loss evaluation for these flaws is valid.

For calculating the signal loss of reflected and transmitted ultrasonic waves from double random rough interfaces, we selected copper blocks as the solid specimen materials. We supposed that the specimens were made from welding of tow copper blocks, in which the top surface above the

Table I. Parameters and data for calculation.

Items	Data
Sound velocity in water	1500 m/s
Sound velocity in copper	4700 m/s
Transducer radius	6 mm
Autocorrelation length of the rough surface	0.8 mm

welding seam is random rough surface, and the rough flaw lies in the welding seam between two copper blocks. The numerical data for calculation are provided in Table I.

The relationships of the incident angle of acoustic waves and the signal attenuation with different flaw depth d are shown in Figure 4, in which the upper and lower interfaces (flaw surface) are both rough interfaces. Seen from the plot, the signal attenuation is obviously affected by the ultrasonic wave incident angle when the flaw depth is in the range from 1 to 4mm. This means that the signal attenuation will decrease along with the increase of the incident angle. When the incident angle reaches 10°, the attenuation turns to minimum. The attenuation will increase along with the increase of the incident angle till reaching a critical angle about 18.6° at which the wave transform will occur and the longitudinal waves will disappear. It shows that the rough interface will enhance the diffuse scattering energy and weaken the specular energy for the oblique incident wave at a large angle. As the flaw depth is 5mm, the signal attenuation is not sensitive to the incident angle, and the variation of the attenuation with the incident angle more than 10° is similar to the one for the flaw near the upper interface. This result shows that the influence of the angle factor on the phase correlation for the waves doubly transmitted through the rough interface will only operate at near upper interface. And the signal attenuation for the oblique incident wave at large angle is related to the distribution of the scattering wave.

Figure 5 presents the relationship between the flaw depth and the signal attenuation with different incident angle of acoustic waves. It shows the less the incident angle, the more the attenuation with a slow changing tendency when the flaw depth is small, while for the large oblique incidence, the attenuation decrease rapidly to a constant value. The attenuation will no longer be dependent on the incident angle (within the critical angle) and reach a constant value when the flaw depth is over 5 mm.

In respect to the trends of the signal attenuation varying with the frequency, only a small difference exists for the small incident angles of acoustic waves, while consistence will be reached for the large incident angles, as shown in Figure 6.

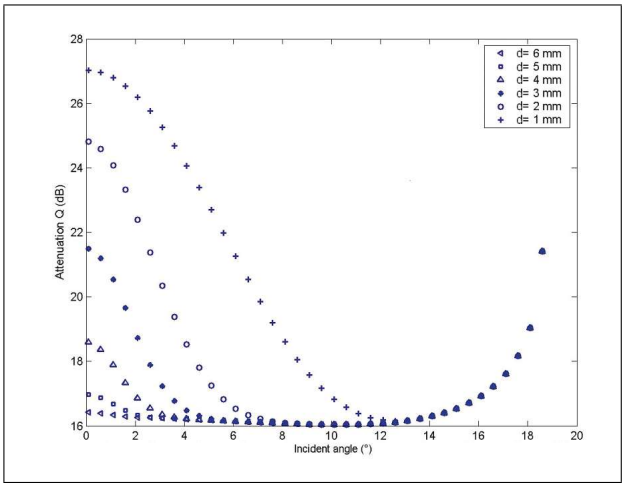


Figure 4. The incident angle of acoustic waves and the signal attenuation ($f = 10\,\text{MHz}$, $h = 40\,\mu\text{m}$).

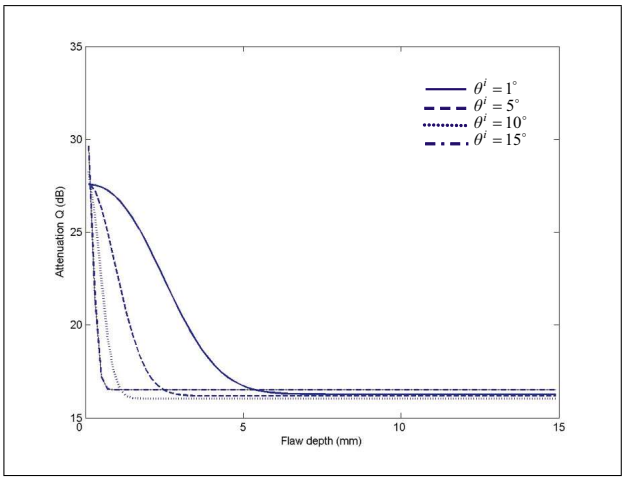


Figure 5. The flaw depth and the signal attenuation ($f = 10\,\text{MHz}$, $h = 40\,\mu\text{m}$).

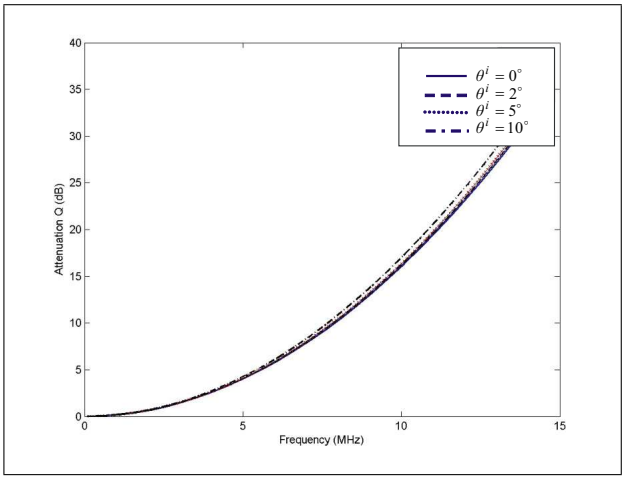


Figure 6. The frequency and the signal attenuation ($h = 40\,\mu\text{m}$).

5. Experiment

The ultrasonic imaging testing systems, shown as Figure 7, were used in this paper for the experimentally evaluating the signal loss induced by double rough interfaces. An unfocused immersion transducer with radius of 6 mm, a central frequency of 10 MHz and a band-width of 5 MHz were chosen in the systems. The sensitivity of the ultrasonic pulser and the receiver is 0.5 dB. The effect of the flaw de-

tection in the materials is mainly determined by the signal loss of coherent waves induced by rough interfaces. The total signal loss of planar waves from non-focused transducer is related to the interface roughness and the correlation of acoustic waves doubly propagating through the rough interface.

Using twenty four 20 mm × 20 mm × 5 mm (thickness) copper blocks to fabricate the specimens, we calculated and experimentally measured the influence of the rough surface on the flaw signal. All blocks were milled and then polished on both sides to make smooth, flat and parallel surfaces. The blocks were divided into three groups and were further processed into two sets of specimens. The surface RMS roughness data are listed in Table II.

Six blocks in Group 1 were processed with blasting shot on one side (lower surface) to make rough surfaces with different roughness with the other side (upper surface) kept smooth . Another six blocks in Group 2 were processed with blasting shot on one side (upper surface), to make rough surfaces with same roughness and were processed with blasting shot on the other side (lower surface) to make rough surfaces with different roughness . Of course, the corresponding roughness of lower surface from Group 1 is same as that of Group 2. In Group 3, both sides of the twelve blocks on the left were kept smooth. Then, use 2mm thick waterproof double-sided adhesives to mate Group 1 blocks one by one with six Group 3 blocks to make the first set of specimens. Likewise, form the second set of specimens by mating Group 2 blocks one by one with the rest six Group 3 blocks. The diagram of complete specimen is shown in Figure 8, where the flaw is used for simulating poor penetration of soldering.

A precision surface profilometry (PE2000) is used to measure the surface roughness. The data acquired from the profilometry is processed by the fast Fourier transform and the high-pass filter to get accurate surface parameters including rms roughness and the autocorrelation length. With a definite thickness of the sample, the pulses needed in the experiments can be ensured in the analysis range by modulating the time-gate of the oscillograph so as to trace the flaw signals. However, the experiment precision is not high enough relative to the special average, because the uncertainty of the tiny time arriving will result in the signal distortion so as to blur the signal's characteristics, such as the decrease of high frequency quantum of the signals. In fact, the adverse effect is resulted from tiny variations of the sample thickness. The effect can be solved by the cross correlation method to maximize the correlation of the testing signal with referenced signal achieved form the wave of the transducer center. In fact, the aim of the process is to eliminate the planar low frequency quantum of some signals resulted from that the correlation length is more than transducer diameter.

By varying rms height of the flaw rough interface, the comparisons of measured results and the values of theoretical prediction are shown in Figures 9–12. The results show a good consistency of the experiments and the theory, especially for rms roughness less than. The maximal

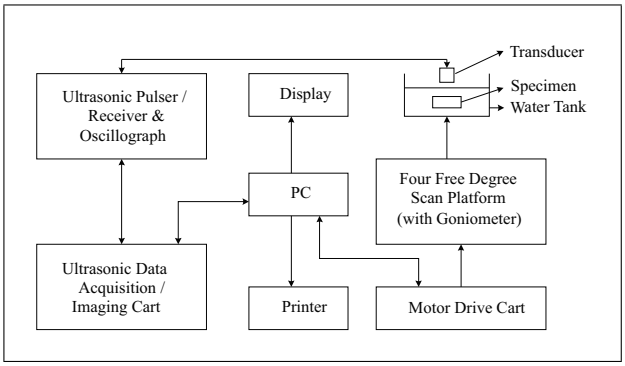


Figure 7. Diagram of the ultrasonic imaging testing system.

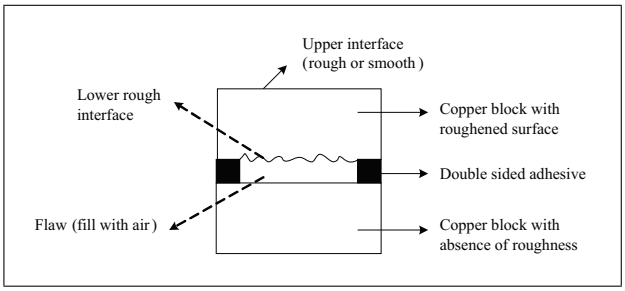


Figure 8. Specimen diagram.

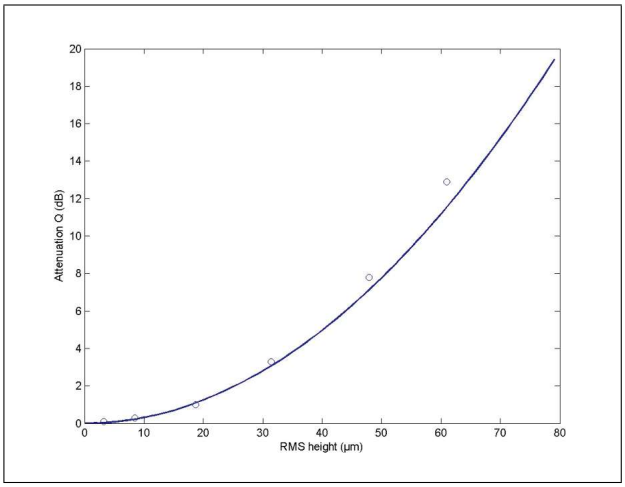


Figure 9. The plot of rms height vs the attenuation using the first group of specimens (where the upper interfaces are smooth, $f = 10\,\mathrm{MHz}$, $L_a = 0.8\,\mathrm{mm}$, the incident angle is 0°, and the solid line denotes the theoretical prediction, the dotted data are from experimental measurements).

error between measured results and theoretical prediction at the point of of rms roughness is still lower than 10% (2.5 dB) (see Figure 10). Therefore the theoretical prediction can meet the needs of the rough flaw detection under rough surfaces for NDT.

6. Conclusion

A model evaluating the signal loss of reflected and transmitted ultrasonic waves induced by double random rough interfaces was presented based on Phase-Screen approx-

Table II. The data of rms roughness of lower surfaces.

Group No.	Position of surface in block	1#	2#	3#	4#	5#	6#
Group 1	RMS roughness of upper surface (μm)	0	0	0	0	0	0
	RMS roughness of lower surface (μm)	3.2	8.5	18.7	31.4	47.9	61.0
Group 2	RMS roughness of upper surface (μm)	41.5	41.5	41.5	41.5	41.5	41.5
	RMS roughness of lower surface (μm)	3.2	8.5	18.7	31.4	47.9	61.0
Group 3	Upper surface Lower surface	Both sides of the twelve blocks were kept smooth					

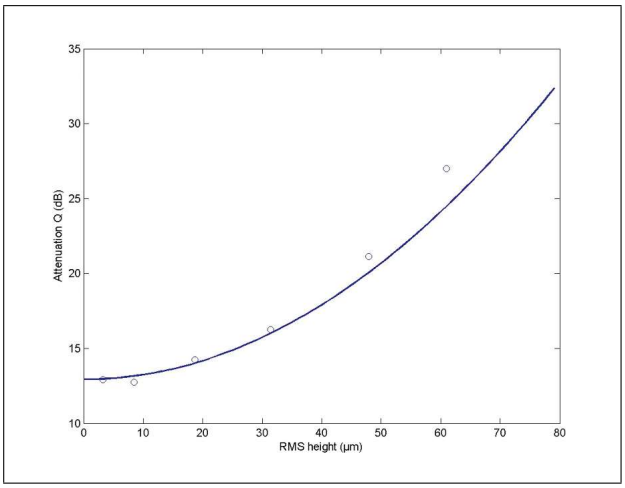


Figure 10. The plot of rms height vs. the attenuation using specimens in Group 2 (where the rms height of upper interface is 41.5 μm, $f = 10$ MHz, $L_a = 0.8$ mm, the incident angle is 0°, and the solid line denotes the theoretical prediction, the dotted data are from experimental measurements).

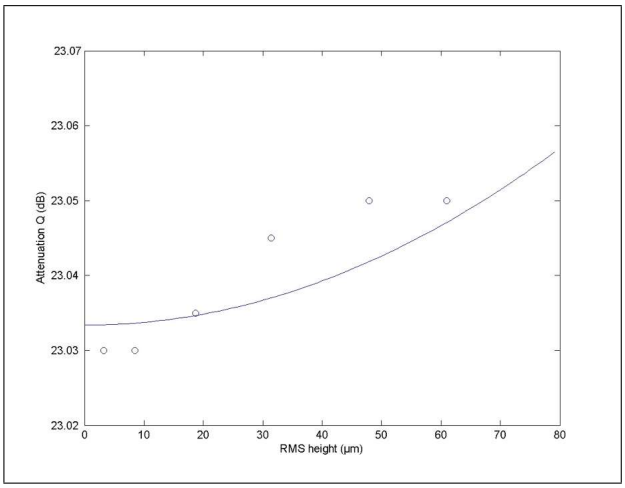


Figure 12. The plot of rms height vs. the attenuation using specimens in Group 2 (where the rms height of upper interface is 41.5 μm, $f = 10$ MHz, $L_a = 0.8$ mm, the incident angle is 18.6°, and the solid line denotes the theoretical prediction, the dotted data are from experimental measurements).

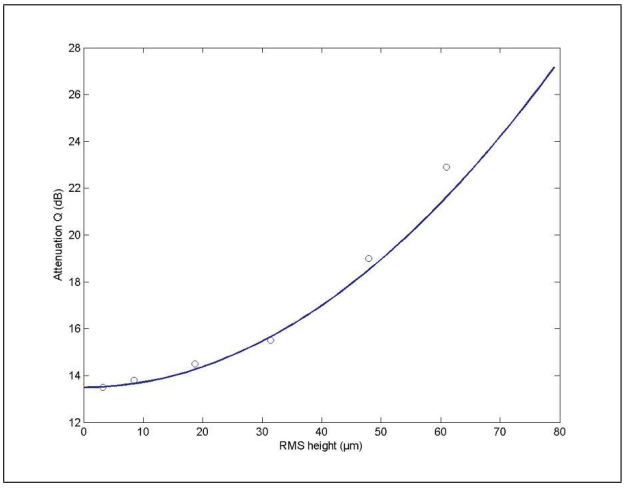


Figure 11. The plot of rms height vs. the attenuation using specimens in Group 2 (where the rms height of upper interface is 41.5 μm, $f = 10$ MHz, $L_a = 0.8$ mm, the incident angle is 10°, and the solid line denotes the theoretical prediction, the dotted data are from experimental measurements).

imation (PSA). In the model, the phase correlation factor of the acoustic beam doubly transmitted through the rough interfaces was expressed into the function of the flaw depth and the incidence angle. Therefore the model overcomes some limitations and inadequacy subjected by those models in which only the phase-screen approximation is used to evaluate the signal loss of the single rough interface.

The signal attenuation will decrease with the increase of the incident angle for the flaw near upper interface, while the signal attenuation is not sensitive to the incident angle as the flaw is far from the upper interface. The results indicate that the influence of the angle factor for the waves doubly transmitted through the rough interface on the phase correlation will only operate at near upper interface. Meantime, the less the incident angle is, the more the attenuation will be with a slowly changing tendency when the flaw depth is small, while for the large oblique incidence, the attenuation decrease rapidly to a constant value. The attenuation will no longer be dependent on the incident angle (within the critical angle) and reach a constant value when the flaw is far from the upper interface (such as 5mm in the paper).

The experimental results show that the values of theoretical prediction are in well agreement with the measured results. Therefore, the model proposed in the paper is suitable for real-time ultrasonic NDT or NDE of rough flaws under the rough surfaces in materials.

Acknowledgement

The authors would like to express their thankfulness to the support of SJTU-NEC jointed lab. The authors would also like to express their appreciation and gratitude to the editors and reviewers for their valuable comments.

References

[1] J. E. Wilhjelm, P. C. Pedersen, S. M. Jacobsen: The influence of roughness, angle, range, and transducer type on the echo signal from planar interfaces. IEEE Trans. Ultrason., Ferroelect., Freq. Contr. **48** (2001) 511–521.

[2] Z. Q. Chen, C. Z. Ni, L. G. Chen, J. Xue: Diffraction of ultrasonic waves from periodic solid-gas rough surfaces in electric contact weld. Acta Acustica united with Acustica **87** (2001) 333–339.

[3] N. F. Declercq, J. Degrieck, R. Briers, O. Leroy: Diffraction of homogeneous and inhomogeneous plane waves on a doubly corrugated liquid/solid interface. Ultrasonics **43** (2005) 605–618.

[4] P. Wu: Nonlinear interaction of ultrasound with an unbounded rough interface. IEEE Ultrasonics Symposium, 2005, 289–292.

[5] P. C. Pedersen, A. Grebe: Application of time delay spectrometry for rough surface characterization. Ultrasonics **39** (2001) 101–108.

[6] K. G. Sabra, P. Roux, H. C. Song, W. S. Hodgkiss, W. A. Kuperman: Experimental demonstration of iterative time-reversed reverberation focusing in a rough waveguide. Application to target detection. J. Acoust. Soc. Am. **120** (2006) 1305–1314.

[7] M. D. Billy, F. Cohen-Tenoudji, G. Quentin, K. Lewis, L. Adler: Ultrasonic evaluation of geometrical and surface parameters of rough defects in solids. J. NDE **40** (1980) 294–261.

[8] B. Morvan, A. C. H. Hennion, D. Leduc, J. L. Izbicki: Ultrasonic guided waves on a periodical grating: Coupled modes in the first Brillouin zone. J. Appl. Phys. **101** (2007) 114906.

[9] K. Kudo, H. Hasegawa, H. Kanai: Measurement of angular dependence of ultrasonic echo for estimation of surface roughness. Jpn. J. Appl. Phys. **46** (2007) 4873–4880.

[10] P. Ratilal, M. Andrews, N. Donabed, A. Galinde, C. Rappaport: Model for continuously scanning ultrasound vibrometer sensing displacements of randomly rough vibrating surfaces. J. Acoust. Soc. Am. **121** (2007) 863–878.

[11] J. Y. Kim, J. S. Lee: A micromechanical model for nonlinear acoustic properties of interfaces between solids. J. Appl. Phys. **101** (2007) 043501.

[12] C. Potel, D. Leduc, B. Morvan, C. Depollier, A. C. Hiadky-Hennion, J. L. Izbicki, P. Pareige, M. Bruneau: Lamb wave attenuation in a rough plate. I. Analytical and experimental results in an anisotropic plate. J. Appl. Phys. **104** (2008) 074908.

[13] C. Potel, D. Leduc, B. Morvan, C. Depollier, A. C. Hiadky-Hennion, J. L. Izbicki, P. Pareige, M. Bruneau: Lamb wave attenuation in a rough plate. II. Analytical and numerical results in a fluid plate. J. Appl. Phys. **104** (2008) 074909.

[14] P. B. Negy, L. Adler: Surface toughness induced attenuation of reflected and transmitted ultrasonic waves. J. Acoust. Soc. Am. **82** (1987) 193–197.

[15] P. B. Negy, J. H. Rose: Surface roughness and the ultrasonic detection of subsurface scatterers. J. Appl. Phys. **73** (1993) 566–580.

[16] P. B. Nagy, L. Adler. – In: Review of Progress in Quantitative Nondestructive Evaluation. D. O. Thompson, D. E. Chimenti (eds.). Plenum, New York, 1988, 1263–1271.

[17] P. Beckmann, A. Spizzichino: The scattering of electromagnetic waves from rough surfaces. Pergamon Press, 1963.

[18] W. A. Kurperman, H. Schmidt: Rough surface elastic wave scattering in a horizontally stratified ocean. J. Acoust. Soc. Am. **79** (1986) 1767–1777.